

# Prototype Detector for Ultrahigh Energy Neutrino Detection<sup>†</sup>

Joshua R. Klein\* and Alfred K. Mann\*\*

Department of Physics & Astronomy

University of Pennsylvania<sup>‡</sup>

Philadelphia, PA 19104

May 27, 1998

Abstract

Necessary technical experience is being gained from successful construction and deployment of current prototype detectors to search for UHE neutrinos in Antarctica, Lake Baikal in Russia, and the Mediterranean. The prototype detectors have also the important central purpose of determining whether or not UHE neutrinos do in fact exist in nature by observation of at least a few UHE neutrino-induced leptons with properties that are not consistent with expected backgrounds. We discuss here the criteria for a prototype detector to accomplish that purpose in a convincing way even if the UHE neutrino flux is substantially lower than predicted at present.

---

<sup>†</sup> Submitted to *Astroparticle Physics*

\* jrk@upenn5.hep.upenn.edu

\*\* mann@dept.physics.upenn.edu

<sup>‡</sup> Supported in part by the U.S. Department of Energy

## Introduction

There are several current efforts to construct deeply buried particle detectors of very large dimensions with which to search for ultrahigh energy (UHE) neutrinos from space [1]. These efforts involve prototype detectors aimed at mastering equipment design and techniques for deployment in ice or in deep water. The sensing elements to detect the leptonic products of UHE neutrino interactions in the vicinity of the detector are photomultiplier tubes (PMTs) and their associated circuitry which present new technical problems of power capacity and distribution and of data acquisition insofar as the PMTs are deployed at a large distance from the power source and in an unusual medium. Deployment in ice or in the sea, particularly the deep sea, requires development of new designs[2],[3] and of an infrastructure new to particle physicists. These issues need to be studied empirically by the experience that the prototype detectors are meant to provide.

However, the prototype detectors have an important physics purpose in addition to answering the technical questions above. This purpose is to determine whether or not the hypothesized UHE neutrino sources which are the object of the search do in fact exist in nature. Specifically, the purpose of the prototype detectors is to demonstrate the existence of UHE neutrinos by observation of at least a small number of UHE neutrino-induced muons or neutrino-induced electrons with properties that are not consistent with expected, well-understood backgrounds. It is difficult to foresee the construction of a detector much larger than a prototype detector in the absence of such a proof of existence.

In this note we discuss briefly the criteria to be satisfied by a prototype detector to accomplish that purpose in a convincing way. We rely heavily on the valuable, encyclopedic paper of Gandhi et al.[4], but concentrate specifically on the criteria necessary to achieve an UHE neutrino-induced signal above background subject to the perhaps pessimistic assumption that the sought-for UHE neutrino flux is an order of magnitude lower in intensity than the current predicted values. This is not a mindless assumption because the UHE neutrino flux calculations are strongly dependent on the uncorroborated models chosen to simulate the acceleration mechanisms in extragalactic and cosmic sources. A lower than predicted UHE neutrino flux would be similar in intensity to known backgrounds and difficult to extract convincingly from them without rethinking how the search should be performed and how a useful upper limit on the neutrino flux can be obtained. Our aim is to suggest a minimal detector and to indicate how the location and operation of the detector will discriminate against backgrounds and provide a high probability of observing a few UHE neutrino-induced leptons

in one or two years of exposure even if the actual UHE neutrino flux is as much as a factor of ten lower than the predicted values.

### **UHE Neutrino-Induced Muon Rates and Angular Distributions**

Interest in a search for UHE neutrinos from space lies in the possibility that astronomical or cosmological sources might give rise to neutrinos in the energy region between  $10^6$  GeV and  $10^{12}$  GeV. That is the energy region in which attempts to model power generating mechanisms involving black holes and accretion disks in active galactic nuclei (AGN) yield observable UHE neutrinos fluxes [5], as do also models of relativistic fireballs for gamma-ray bursters (GRBs) [6]. Various conjectures in elementary particle and cosmological theory introduce so-called topological defects (TDs) that give rise to the decays of very massive remnant particles, one of whose decay products might be an UHE neutrino [7]. A summary of the results of these model-based calculations of neutrino fluxes—which we take as order of magnitude estimates—is given in Fig. 1.

It is realistic to consider the prospect of observing the low intensity fluxes in Fig. 1 because the reaction cross section for neutrino plus nucleon rises steeply with neutrino energy as shown in Fig. 2 for both neutrinos and antineutrinos [4]. Observe that the cross section rises by roughly six decades as the neutrino energy increases by eight decades from 1 GeV to  $10^8$  GeV, despite the production of real intermediate vector bosons as indicated by the breaks in the curves in Fig. 2 at about  $10^5$  GeV.

A further consequence of the rapid increase of neutrino interaction cross sections is that the Earth becomes a significant absorber of neutrinos above a certain neutrino energy, roughly  $10^4$  GeV, and is essentially opaque to neutrinos with energy above about  $10^7$  GeV. The neutrino survival probability as a function of  $\cos\theta_Z$ ,  $\theta_Z$  the zenith angle at the detector, for three neutrino energies is plotted in Fig. 3. This well-understood effect is particularly damaging because the angular region in which one naturally thinks to search for leptons from UHE neutrino interactions near or in a massive detector is the region  $\cos\theta_Z \lesssim 0$ . This effect requires some revision of most current plans for UHE neutrino searches, particularly if they are to search successfully for UHE neutrino interaction products from a neutrino flux significantly lower than is shown in Fig. 1.

To estimate the differential flux  $d\phi_\mu^\nu/d\Omega$  of UHE neutrino-produced muons from neutrinos in the energy interval  $10^7$  to  $10^{10}$  GeV reaching a detector at a depth of 5 km.w.e., we numerically integrate over neutrino energy and all possible neutrino interaction points in the Earth ( $X$ ), weighted by the neutrino interaction probability and the probability of muon

survival over a distance from  $X$  to the detector position ( $D(\cos \theta_z)$ ):

$$\frac{d\phi_\mu^\nu}{d\Omega} = \int \frac{d\phi_\nu}{dE_\nu d\Omega} \int_0^{D(\cos \theta_z)} \sigma_{\nu N}(E_\nu) n e^{-\sigma_{\nu N}(E_\nu) n X} \int P_{\text{surv}}^\mu(E_\mu, D(\cos \theta_z) - X) \left( \frac{1}{\sigma_{\nu N}} \frac{d\sigma_{\nu N}}{dE_\mu} \right) dE_\mu dX dE_\nu \quad (1)$$

We choose the representative UHE neutrino energy interval  $10^7$  to  $10^{10}$  because  $10^7$  GeV is roughly the lowest energy at which it is likely that new physics can be convincingly identified by the experimental method discussed here and, on the other hand, observation of muons from  $10^{10}$  GeV neutrinos would unquestionably signify new physics. We use the values calculated by Gandhi *et al.* [4] for the total neutrino-nucleon cross section  $\sigma_{\nu N}(E_\nu)$  and the Monte Carlo results of Lipari and Stanev [8] for the muon survival probability  $P_{\text{surv}}^\mu$ . The differential neutrino flux is taken from the values shown in Fig. 1. For simplicity, we replace the differential cross section for muon production with a delta function centered on half the incident neutrino energy, i.e.,

$$\frac{1}{\sigma_{\nu N}} \frac{d\sigma_{\nu N}}{dE_\mu} = \delta\left(E_\mu - \frac{1}{2}E_\nu\right)$$

which reduces Equation 1 to

$$\frac{d\phi_\mu^\nu}{d\Omega} = \int \frac{d\phi_\nu}{dE_\nu d\Omega} \int_0^{D(\cos \theta_z)} \sigma_{\nu N}(E_\nu) n e^{-\sigma_{\nu N}(E_\nu) n X} P_{\text{surv}}^\mu\left(\frac{E_\nu}{2}, D(\cos \theta_z) - X\right) dX dE_\nu. \quad (2)$$

This substitution is adequate for the order of magnitude estimates we present here. Implicit in Equation 1 is the assumption that the muons are produced collinearly with the neutrinos, that is,  $d\sigma_{\nu N}/d\Omega$  is a delta function centered on the incident neutrino direction.

In Figure 4a, we plot the UHE neutrino-induced muon flux as a function of detector zenith angle  $\cos \theta_z$ , for a detector 5 km deep and for three different incident neutrino energies to give an idea of the energy dependence within the interval  $10^7$  to  $10^{10}$  GeV. As is evident, there are three distinct regions for each curve. For  $\cos \theta_z < -0.10$ , the muon flux drops off rapidly—a consequence of the extreme attenuation of the neutrino flux shown in Fig. 3. For  $\cos \theta_z > 0.25$ , the flux drops somewhat less rapidly because the neutrino target thins, resulting in fewer neutrino interactions and fewer muons. Between those limits, the neutrino target thickness is small compared to the neutrino interaction length but greater than the muon range. Thus the UHE neutrino flux is unattenuated, and all neutrino interactions closer to the detector than the muon range yield detected muons. This maximum detected muon flux does not change until the neutrino target thickness becomes smaller than the muon range, at  $\cos \theta_z > 0.25$ .

These general features, which are largely the result of the geometry of the experimental arrangement, can be confirmed with an even simpler model. If we take the muon range at these energies to be roughly 20 km.w.e., then the only neutrino interactions that produce detectable muons occur within 20 km.w.e. of the detector. The total number of neutrino interactions in a target of thickness  $D$  is just  $\phi_\nu[1 - \exp(-\sigma_\nu N(D))]$ , of which only  $20\text{km.w.e.}/D$  produce detectable muons. So, for example, for a neutrino flux at  $10^7$  GeV of  $10^{-4}(\text{km}^{-2}\text{s}^{-1}\text{sr}^{-1})$ , and a cross section of  $10^{-33}\text{cm}^2$ , we find at  $\cos\theta_z = 0.1$  a muon flux of  $\sim 3 \times 10^{-7}(\text{km}^{-2}\text{s}^{-1}\text{sr}^{-1})$ , in good agreement with the full integral calculation above. In this model, for  $\cos\theta_z > 0.25$  the flux drops as  $[1 - \exp(-\sigma_\nu N(D))]/[1 - \exp(-\sigma_\nu N(20))]$  as the maximum distance to the detector becomes less than the 20 km.w.e range.

In either of these models, the width of the region of maximum detected muon flux is a strong function of detector depth. We plot in Figure 4b the angular distribution of the UHE neutrino-induced muon flux as a function of  $\cos\theta_z$  for a detector at a depth of 2 km.w.e., which shows a steeper fall-off of the acceptance region at small zenith angles as the detector moves closer to the surface. To obtain the relative UHE neutrino-induced muon intensities for the two detector depths in Fig. 4, it is necessary to take into account the angular limits imposed by the large cosmic ray muon flux, which are different for the different detector depths as discussed in the next section. These limits are indicated in Fig. 5 with the UHE neutrino-induced fluxes integrated over the energy interval  $10^7$  to  $10^{10}$  GeV for each of the detector depths. Summing the UHE-induced muon flux from the cosmic ray muon limits to  $\cos\theta_z \simeq -0.10$  yields the UHE neutrino-induced muon flux at a detector depth of 5 km integrated over the solid angle acceptance of the detector to be approximately  $I_\mu^\nu = 5.3 \times 10^{-6}\text{km}^{-2}\text{sec}^{-1}$ , and the ratio of the induced muon fluxes at 5 km and 2 km to be 1.7.

## Backgrounds

Apart from the serious technical difficulties involved in working deep under ice or under the sea, the primary obstacle to achieving a convincing demonstration of the observation of an UHE muon from an UHE neutrino source in space is background from two known sources of energetic muons; cosmic ray muons in Fig. 5 coming directly from primary cosmic ray proton (and heavier element) interactions in the Earth's atmosphere, and muons produced by the cosmic ray (often called atmospheric) neutrinos that are the birth companions of the cosmic ray muons. These empirically well-studied backgrounds fall off rapidly with increasing muon energy, but their energy distributions have long tails extending past  $10^7$  GeV. This is

shown for the cosmic ray muons in Fig. 6 [9] which is a companion to the muon plots in Fig. 5, and for the atmospheric (atmos) neutrinos (not muons) in Fig. 1 [10].

### Cosmic Ray Muon Background

As indicated in Fig. 4, the zenith angular interval in which to search efficiently for an UHE neutrino signal in a 5 km deep detector is  $-0.10 \lesssim \cos\theta_Z \lesssim 0.25$ . Cosmic ray muons reaching the detector with  $\cos\theta_Z \lesssim 0.25$  must first traverse at least 20 km w.e.; this requires an incident cosmic ray muon energy of about  $10^8$  GeV for a muon detector energy threshold of  $10^3$  GeV, and  $10^9$  GeV for a muon detector threshold of  $10^4$  GeV. For either energy threshold the cosmic ray muon flux satisfying the angle and energy criteria is roughly  $10^{-17}(\text{km}^{-2}\text{sec}^{-1}\text{sr}^{-1})$ . For comparison, note that cosmic ray muons reaching a 2 km deep detector with  $\cos\theta_Z \lesssim 0.25$  need only traverse 8 km w.e., which requires an incident muon energy of  $10^6$  GeV for a detector energy threshold of  $10^4$  GeV, and is satisfied by the much larger cosmic ray muon flux of about  $5 \times 10^{-7}(\text{km}^{-2}\text{sec}^{-1}\text{sr}^{-1})$ . As a consequence, the angular limit to the acceptance region of a 2 km deep detector is approximately at  $\cos\theta_Z = +0.10$ , where the cosmic ray muon flux is equal to that for a 5 km deep detector at the angular limit  $\cos\theta_Z = +0.25$ . These are the cosmic ray muon limits shown in Fig. 5.

Although the cosmic ray muon flux is small beyond the angular limits in Fig. 5, the steep rise of the flux places a significant demand on the angular resolution of the detector at either depth. To emphasize this fact, the cosmic ray muon fluxes plotted in Fig. 5 are integrated over all energies equal to and above  $10^5$  GeV. One can see graphically that a large, possibly overestimated, lower energy muon background is latent at angles just slightly below the limiting angles shown. For example, a 5 km deep detector with a muon energy threshold of  $10^4$  GeV accepting muons at an angle given by  $\cos\theta_Z = 0.30$  will measure a flux of  $10^8$  GeV cosmic ray muons roughly 100 times larger than the flux at  $\cos\theta_Z = 0.25$ , but still small relative to the UHE neutrino-induced muon flux. However, at  $\cos\theta_Z = 0.30$ , there are approximately 10 times as many lower energy cosmic ray muons as UHE neutrino-induced muons so that the low energy tail on the cosmic ray muon energy distribution will require the 10 TeV detector threshold to eliminate them. On the other hand, angular cuts that are more conservative than those in Fig. 5 clearly eat away at the useful signal. Analogous statements can be made perhaps with greater force for a 2 km deep detector.

### Atmospheric Neutrino-Induced Muon Background

The atmospheric neutrino-induced muon background is more difficult to subdue. In the

interval  $10^5$  to  $10^6$  GeV—a representative energy interval for atmospheric neutrinos (see below)—they produce a muon yield one half as large as the muon yield from UHE neutrinos in the energy interval  $10^7$  to  $10^{10}$  GeV.

However, the different muon energy distributions from the two sources allow them to be differentiated by the 10 TeV energy threshold of the detector. Along the path to the detector, all of the muons from  $10^5$  GeV neutrino interactions in the 2 km segment closest to the detector will pass the energy threshold, as will approximately 2/3 of the muons from the segment of path 2 to 4 km from the detector, and 1/3 from the segment 4 to 6 km away. Few atmospheric neutrino-induced muons originating beyond 6 km will be detected. This is illustrated in Fig. 7, taken from reference [8], which shows the energy distributions of  $10^5$  GeV muons after traversing different lengths of path.

The average energy loss of muons is generally written as  $-dE_\mu/dx = \alpha + \beta E_\mu$ , with  $\beta$  the sum of the fractional radiation losses, which in the high energy limit are proportional to muon energy. In the muon energy region between about  $10^4$  to  $10^9$  GeV,  $\beta$  is weakly dependent on muon energy as indicated in Fig. 8, also taken directly from reference [8]. The result is that the energy loss per unit path length of UHE neutrino-induced  $10^8$  GeV muons is closely  $10^3$  times larger than that for the atmospheric-induced  $10^5$  GeV muons, which in turn means that the shape of the energy distributions in Fig. 7 can be directly scaled to  $10^8$  GeV initial muon energy. Consequently, 95 percent of the muons produced by the UHE  $10^8$  GeV neutrinos in the distant segment of path between 8 and 10 km will clear the threshold and a substantial fraction of the muons from 11 to 20 km would also do so.

The net result of the 10 TeV muon energy threshold is to reduce the detected atmospheric neutrino-induced muon flux by a factor of approximately 5 and yield an UHE signal about 10 times larger than the atmospheric background.

### **Muon Angle and Energy Resolution**

For the muon selection criteria to be effective and discriminate successfully against the cosmic ray muon background, the angular resolution,  $\Delta \cos \theta_Z / \cos \theta_Z$ , of a 5 km deep detector needs to be no worse than 0.2 in the vicinity of  $\cos \theta_Z = 0.25$  and, correspondingly, better than 0.5 for a 2 km deep detector at  $\cos \theta_z \cong 0.10$ . These requirements are significant factors in the design of a prototype detector. For example, assuming a cubic array of photomultiplier tubes (PMTs), the length of an edge of the array and the PMT spacing within the array need to be optimized to achieve the angular resolutions above, while attempting to obtain the area of a side about  $0.1\text{km}^2$  and keeping the cost and deployment problems realistic. This angular

resolution is also satisfactory for the roughly isotropic angular distribution of the atmospheric neutrino background.

Discrimination against atmospheric neutrino-induced muons relies, as we have seen, on the muon energy threshold. The muon yield from  $10^4$  GeV atmospheric neutrinos is 70 times larger than the muon yield from  $10^5$  GeV atmospheric neutrinos. However, the larger muon flux is, on average, below the 10 TeV detector energy threshold even at production and below 1 TeV at the detector entrance. Consequently, the rapidly rising atmospheric neutrino intensity with decreasing neutrino energy is neutralized by the 10 TeV muon threshold. Furthermore, muons from  $10^6$  GeV atmospheric neutrinos are 200 times fewer than the muons from  $10^5$  GeV atmospheric neutrinos.

Accordingly, if the UHE neutrino flux is as large as indicated by present estimates, neither the cosmic ray muon background nor the atmospheric neutrino-induced muon background places an important requirement on the detector energy resolution beyond the 10 TeV threshold cut. If, however, the UHE neutrino flux is as much as an order of magnitude less than anticipated, demands on the energy resolution would become significant. Discrimination against cosmic ray muons by measurement of their incident angle would continue to be sufficient, but a tighter energy criterion might lessen the burden on the angular resolution. On the other hand, a lower UHE neutrino flux would lead to a numerical ratio of UHE neutrino signal to atmospheric neutrino background about equal to unity and require additional discrimination that might be provided by selection criteria reflecting the different energy distributions of the two muon samples as measured within the detector. Detailed study of the observed event distributions, reinforced by Monte Carlo simulations, are likely to allow for statistical separation of the two event samples, but require more detail than is appropriate for this general discussion.

## Summary and Conclusions

To bring to fruition the idea of constructing a detector of sufficient size and capability for an intensive search and detailed study of UHE neutrinos from any source requires first that the existence of such neutrinos be demonstrated conclusively in a smaller, but still quite ambitious detector. The prototype detectors now under design or under construction are directed at that goal, as well as at the task of learning to deploy apparatus and operate in the hostile environments of deep ice or the deep sea.

In this paper we have suggested three correlated operational requirements that a prototype detector should satisfy to achieve that primary physics purpose even if the intensity of the



sought-for UHE neutrinos is an order of magnitude less than estimated at present. First, the prototype detector should be located under as much vertical shielding as possible, preferably about 5 km. Second, analysis of the observed muons should concentrate in the angular region  $-0.10 \lesssim \cos \theta_Z \lesssim 0.25$ ,  $\phi = 2\pi$ , where the UHE neutrinos are not strongly absorbed by the Earth before they produce muons able to reach the detector, and the produced UHE muons will not be outnumbered by the cosmic ray muon flux. Indeed, the vertical depth of the detector provides a slant depth of 20 km at  $\cos \theta_Z = 0.25$  which ensures that the cosmic ray muon background in the interval  $-0.10 \lesssim \cos \theta_Z \lesssim 0.25$  is negligible compared with the pessimistic estimate of the magnitude of the UHE signal we have adopted here, providing the detector angular resolution is adequate. Third, in view of the high energy of the region,  $10^6$  to  $10^{12}$  GeV, in which the search is best conducted and the rapid falloff with energy of the atmospheric neutrino flux, the imposition of a 10 or possibly 20 TeV muon threshold in the data analysis will maintain a numerical ratio of the reduced level of anticipated signal to atmospheric neutrino-induced background to of order unity. To improve this level of discrimination will require statistical separation of the two components of the observing UHE muon energy distribution, which might be achieved in a cubic detector array with linear dimension approximately 0.3 km to absorb a statistically useful sample of energy deposited by the transiting muon. Similar requirements apply to neutrino-induced electrons.

We have given only rough estimated absolute UHE muon signal rates based on the neutrino fluxes in Fig. 1 or fluxes reduced by an order of magnitude because of the large uncertainties involved. Our estimates of the UHE muon signal and the combined background from cosmic ray muons and atmospheric-induced muons suggest, however, that observation of 3 to 10 UHE muons per year with energy greater than  $10^6$  GeV in a detector with geometric area of  $0.1 \text{ km}^2$  is not unlikely, and that these muons would not be confused with background. Such an observation would clearly demonstrate the existence of one or more sources of UHE neutrinos in space or of cosmological origin and justify the construction of a ten or more times larger area detector for detailed study of the new phenomenon.

### Acknowledgements

We are grateful to Todor Stanev for a particularly useful muon range table and a number of discussions, and to T.K. Gaisser and David R. Nygren for discussions. David N. Schramm, always interested in possible new phenomena, was a source of encouragement. Some of these ideas crystallized for one of us (AKM) as a result of witnessing the deployment exercise of a part of the Nestor detector in the Ionian Sea in May, 1997.

## References

1. Antarctica: the Antarctic Muon and Neutron Detector (AMANDA Collaboration) is described by R. Morse, in *Neutrino Telescopes, Proceedings of the Fifth International Workshop, Venice, March 1993*, edited by M. Baldo Ceolin, University of Padua (1993), and by R. J. Wilkes in *Proceedings of the 22nd Annual SLAC Summer Institute on Particle Physics, Stanford, CA (1994)*; P. Askebjær *et al.*, *Science* **267** (1995) 1147.

In the Mediterranean: Proposal to the IN2P3 Scientific Committee by ANTARES Collaboration (1996).

Also in the Mediterranean: the NESTOR project is described by L. K. Resvanis in *Neutrino Telescopes, Proceedings of the Fifth International Workshop, Venice, March 1993*, edited by M. Baldo Ceolin, University of Padua (1993), and in the *Proceedings of the Third NESTOR International Workshop, October, 1993*, edited by L. K. Resvanis, Athens University Press (1994).

Lake Baikal, Russia: The Baikal Neutrino Telescope is described by R. Wischniewski in the *Proceedings of the Third NESTOR International Workshop, October, 1993*, edited by L. K. Resvanis, Athens University Press (1994); I. Sokalski (for the Baikal Experiment) in *Proc. of the Int'l Workshop XXXII Ind Rencontres de Moriond, January, 1997*.

2. The earliest effort to construct a large area neutrino detector in the deep sea from which much was learned was the Deep Underwater Muon and Neutrino Detector (DUMAND). This detector is no longer in operation. It is described in J. G. Learned, *Phil. Trans. Roy. Soc. London A* 346 (1994).

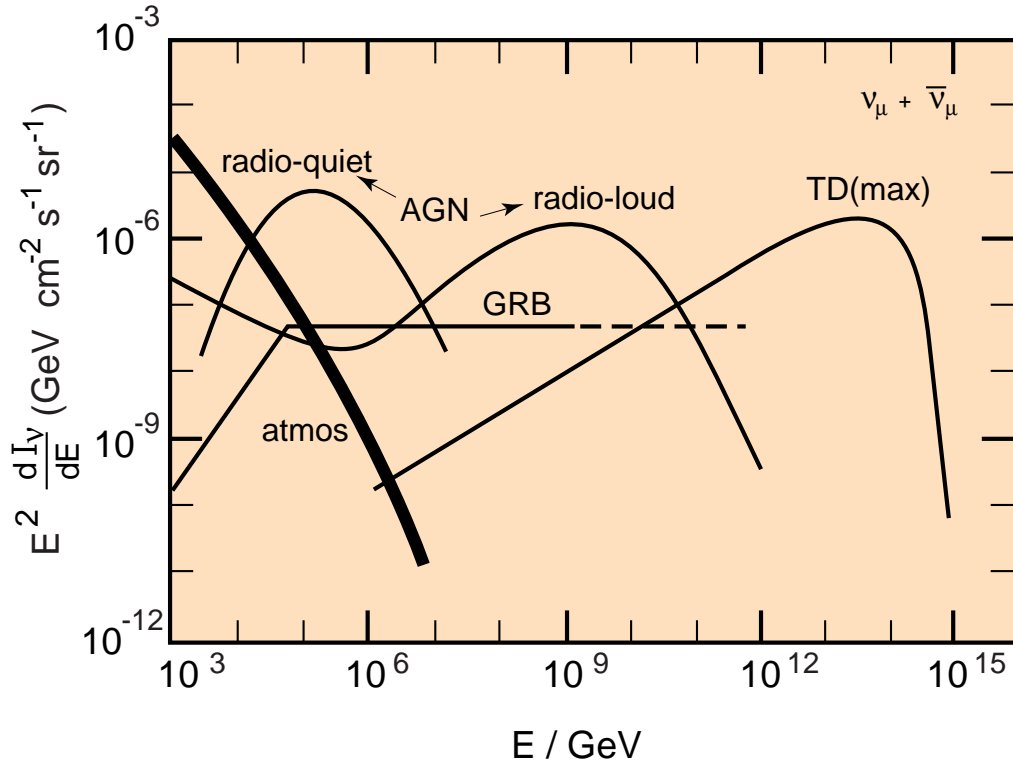
3. For novel detector developments, see D.R. Nygren *et al.* LBL-38321, UC 412.

4. R. Gandhi, C. Quigg, M.H. Reno, and I. Sarcevic, *Astropart. Phys.* **5** (1996) 81; G.C. Hill, *Astropart. Phys.* **6** (1997) 215.

5. Recent estimates of neutrino fluxes from AGN are: L. Nellen, K. Mannheim, and P. L. Biermann, *Phys. Rev.* **D47** (1993) 5270; A.P. Szabo and R.J. Protheroe, *Astropart. Phys.* **2** (1994) 375; K. Mannheim, *Astropart. Phys.* **3** (1995) 295; D. Kazanas in *Proceedings of the Third NESTOR International Workshop, October 1993*, edited by L.K. Resvanis (Athens University Press) 1994; F.W. Stecker and M.H. Salamon, *Space Science Reviews* **75** (1996) 341.

6. E. Waxman and J. Bahcall, Phys. Rev. Lett. **78** (1997) 2292.
7. C.T. Hill, D.N. Schramm and T.P. Walker, Phys. Rev. **D36** (1987) 1007; J.H. MacGibbon and R.H. Brandenberger, Nucl. Phys. **B331** (1990) 153; P. Battacharjee, C.T. Hill and D.N. Schramm, Phys. Rev. Lett. **69** (1992) 567; S. Yoshida and M. Teshima, Prog. Theor. Phys. (Kyoto) **89** (1993) 833; G. Sigl, S. Lee, D.N. Schramm and P. Coppi, Phys. Lett. B (1996); R.J. Protheroe and P.A. Johnson, Astropart. Phys **4** (1996) 253.
8. P. Lipari and T. Stanev, Phys. Rev. **D44** (1991) 3543.
9. S. Hayakawa, Cosmic Ray Physics, John Wiley and Sons, New York (1969).
10. V. Agrawal, T.K. Gaisser, P. Lipari and T. Stanev, Phys. Rev. **D53** (1996) 1314; T.K. Gaisser and T. Stanev, Proc. 24th Int'l Cosmic Ray Conference (Rome, 1995) Vol. 1, p. 694.

Figures



96-0159b-2

6

Fig. 1. Calculated UHE neutrino plus antineutrino fluxes at the Earth's surface weighted by  $E^2$ . See text and reference 5.

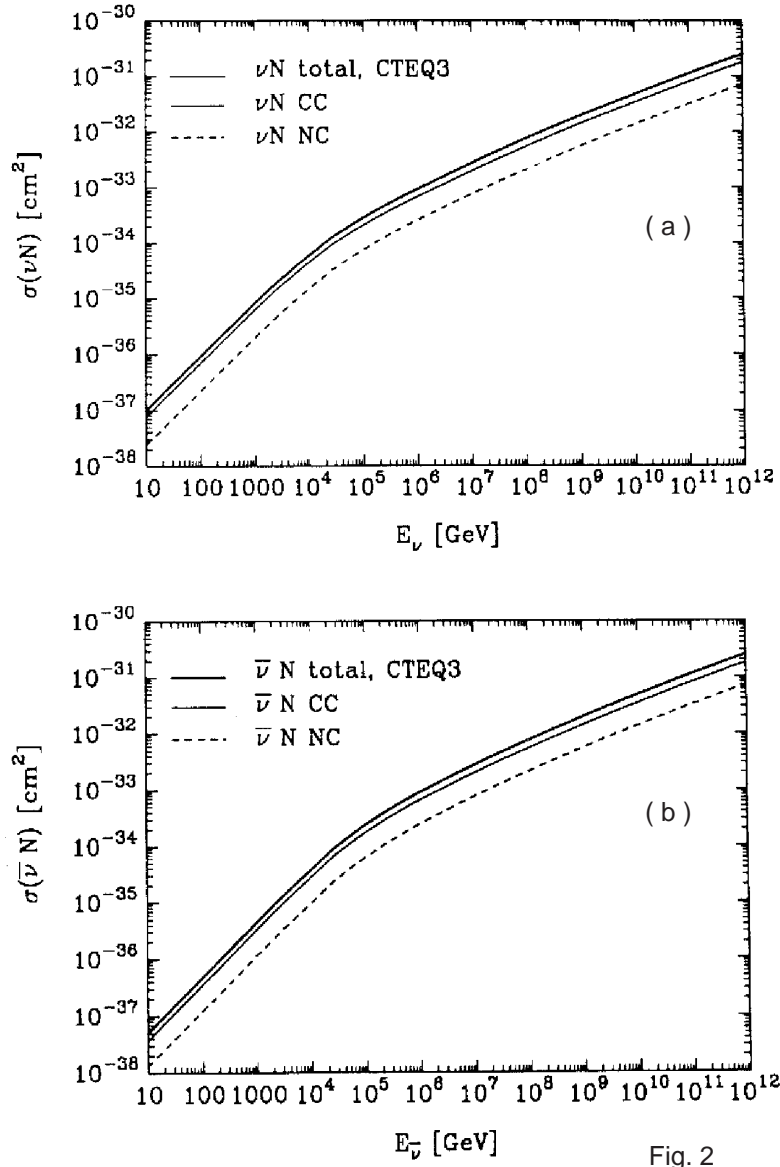


Fig. 2

98-0229h

Fig. 2. Cross sections for (a)  $\nu N$  interactions at high energies; dotted line,  $\sigma(\nu N \rightarrow \nu + \text{anything})$ ; thin line,  $\sigma(\nu N \rightarrow \mu^- + \text{anything})$ ; thick line, total charged-current plus neutral-current) cross section. (b) for  $\bar{\nu} N$  interactions. From reference 4, p. 90.

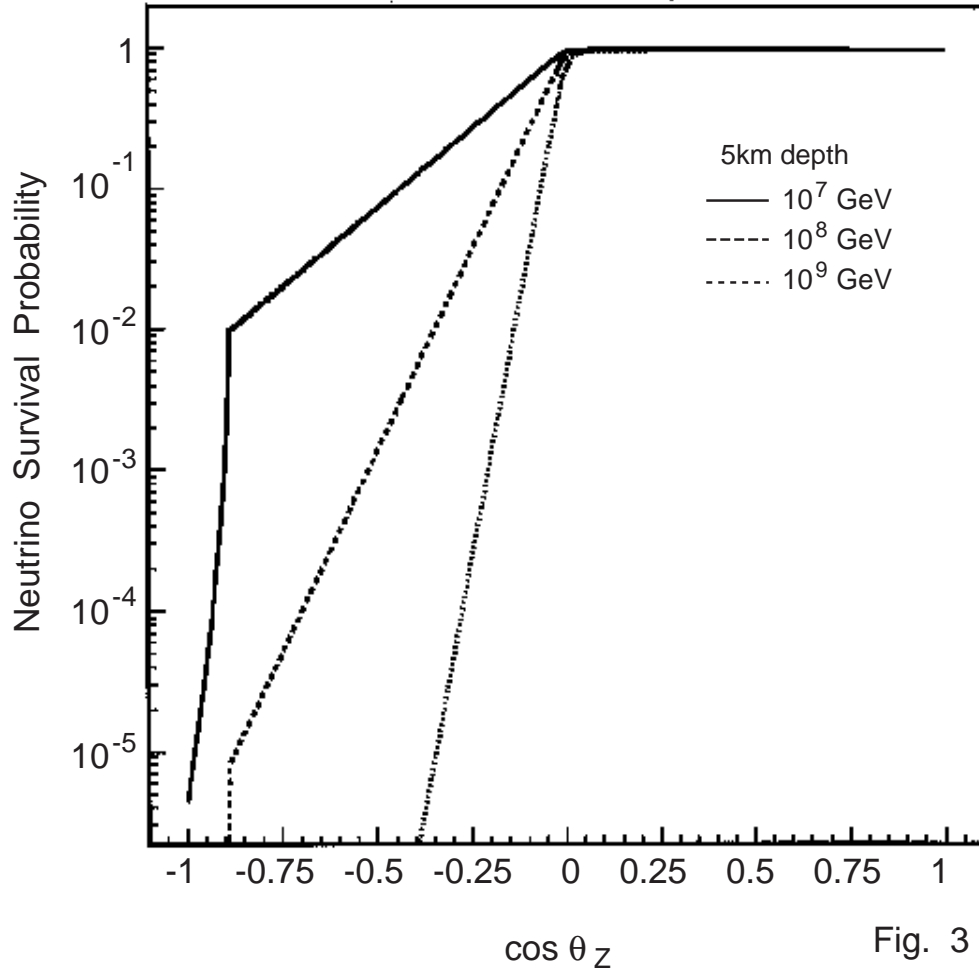


Fig. 3

98-0229i

Fig. 3. Survival probability of UHE neutrinos from space as a function of  $\cos \theta_Z$ , the zenith angle at a detector a few kilometers below the Earth's surface;  $\cos \theta_Z = +1$  corresponds to the zenith direction.

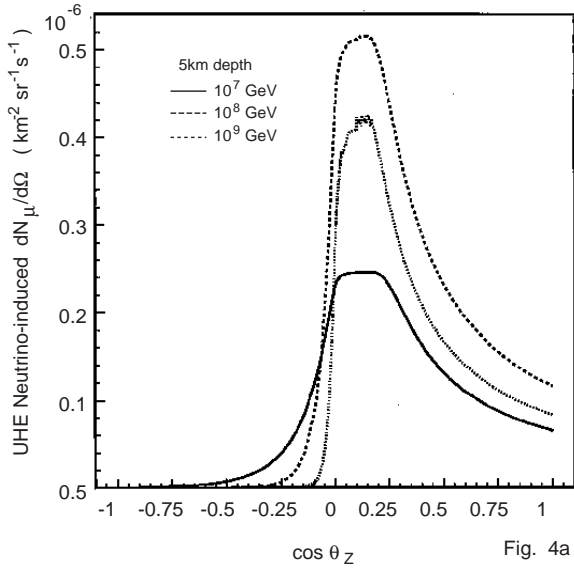


Fig. 4a

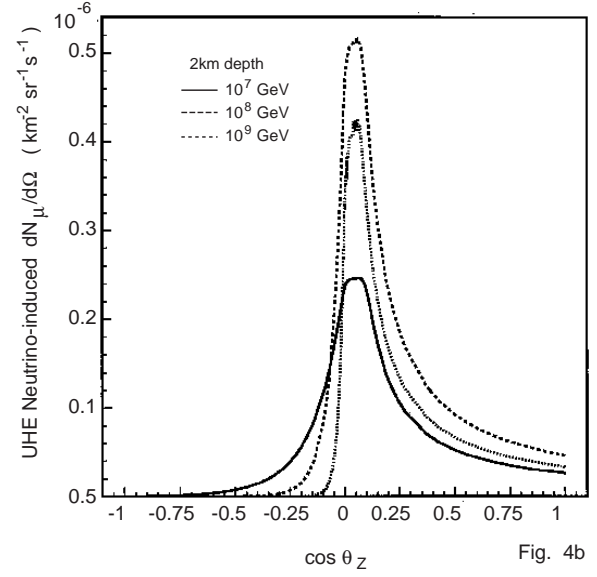


Fig. 4b

98-0226j

98-0226k

Fig. 4. Relative angular distributions of UHE neutrino-induced muons for three neutrino energies in an arbitrary detector located as in the Fig. 3 caption (a) detector 5 km deep, (b) detector 2 km deep.

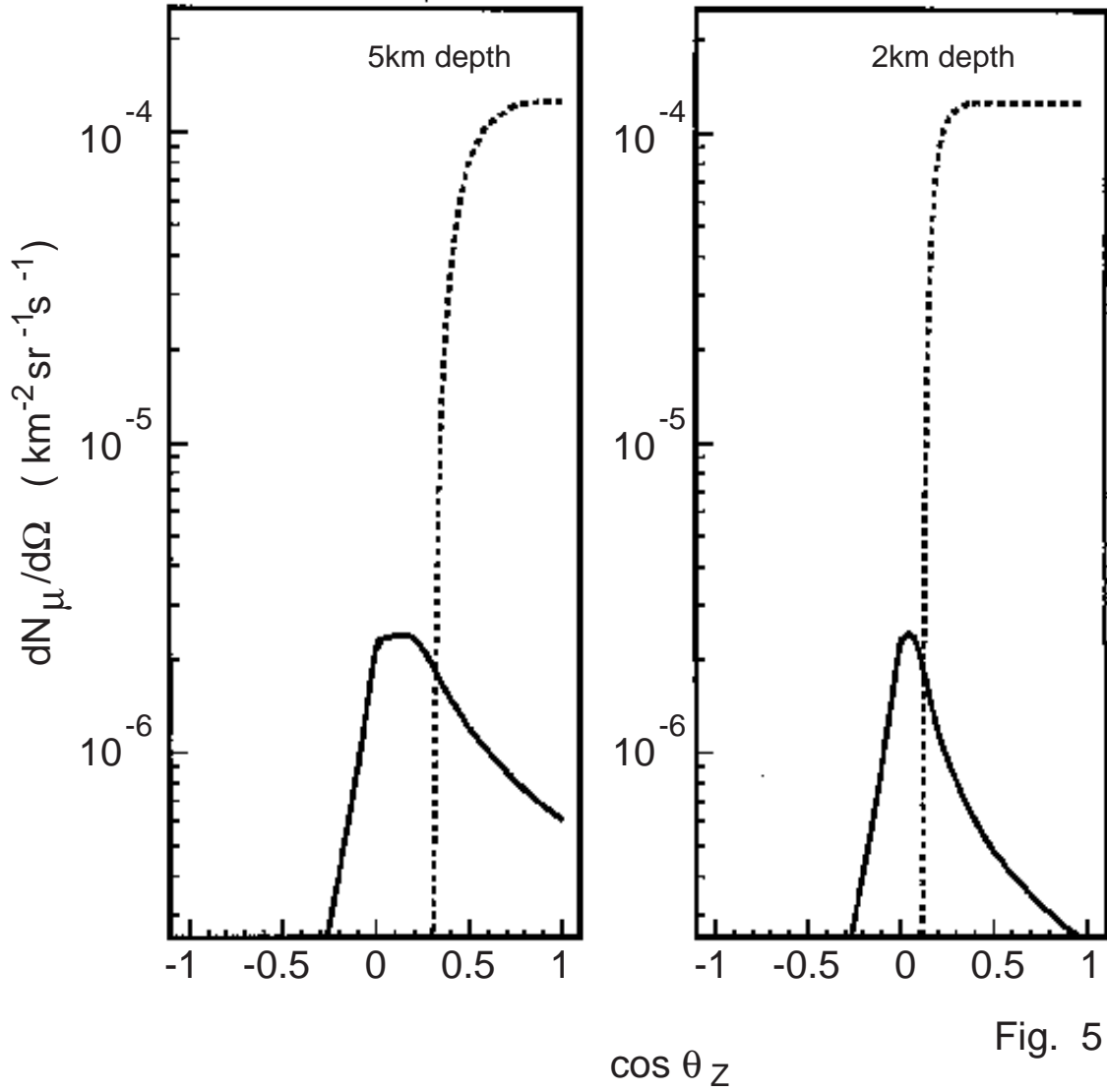


Fig. 5

Fig. 5. The angular distributions of UHE neutrino-induced muons integrated over the energy interval  $10^7$  to  $10^{10}$  GeV with the cosmic ray muon distributions superimposed (a) detector 5 km deep, (b) detector 2 km deep.



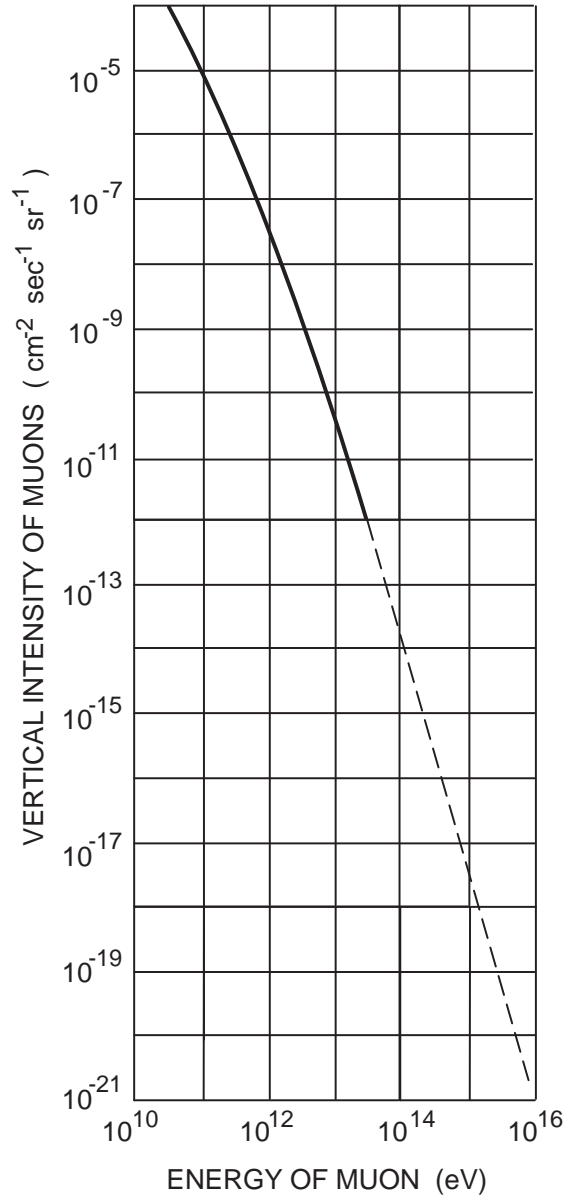


Fig. 6

98-0023a prime

Fig. 6. Integral energy spectrum of cosmic ray muons from reference 8, p. 401. The dashed line is the estimated extrapolation of the original empirically based plot.

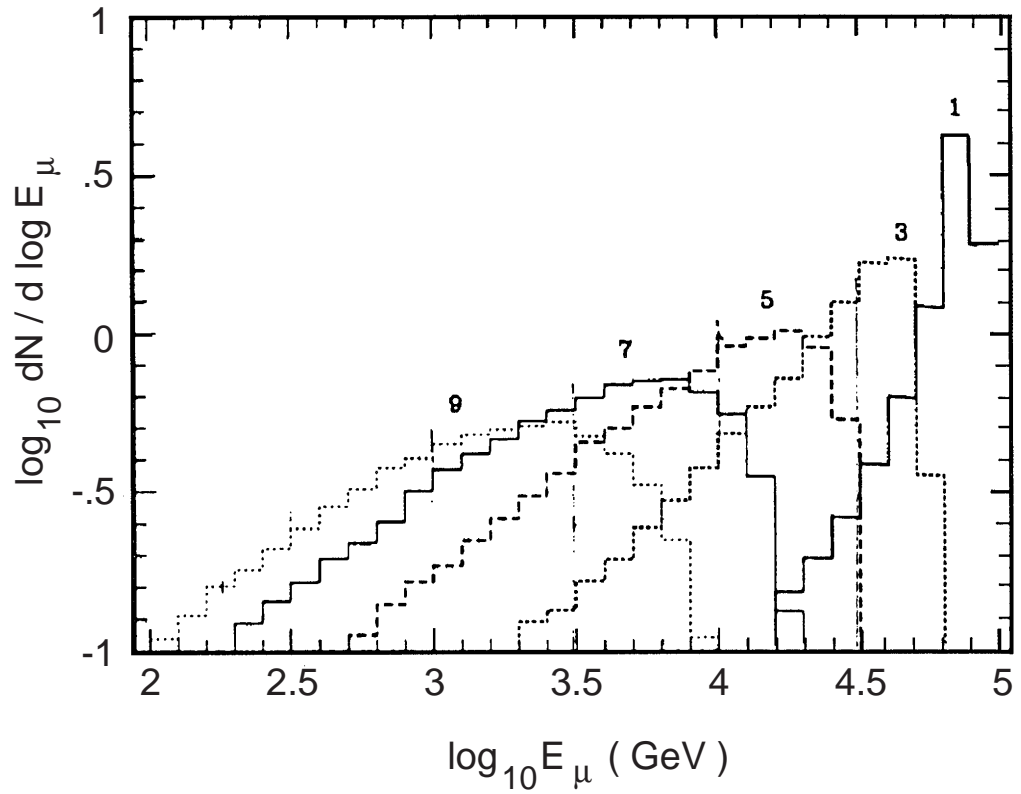


Fig. 7

98-0229g

Fig. 7. Energy distribution of muons of energy  $E_0 = 10^5$  GeV after propagation in standard rock depths from 1 to 9 km w.e. The numbers by the histograms show the corresponding depths. Reproduced from reference [8].

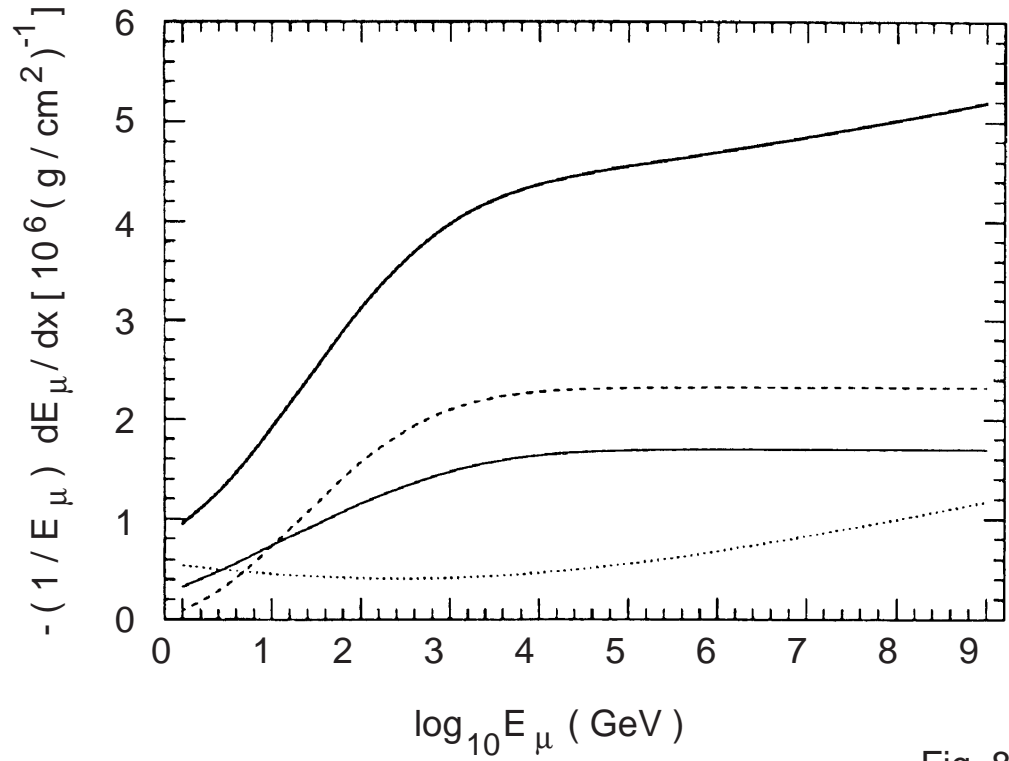


Fig. 8

98-0229e

Fig. 8. Plot of the quantities  $\beta_{rad} = \langle dE/dx \rangle_{rad}/E$  for the three radiative processes in standard rock as a function of muon energy  $E$ . The solid line is for bremsstrahlung, dashed line for production of  $e^+e^-$  pairs, and the dotted line for photoproduction. The thick solid line shows the sum of the three processes. Reproduced from reference [8].